Chiang Mai J. Sci. 2020; 47(6) : 1265-1282
http://epg.science.cmu.ac.th/ejournal/
Contributed Paper

Straightforward Synthesis of (6-methyl-pyridin-2-ylamino)-Acetic Acid from 2-amino-6-methylpyridine and Their Coordination with Copper to Enhance Antibacterial Activity

Husna Syaima [a], Venty Suryanti [a,b] and Sentot B. Rahardjo*[a,b]

[a] Department of Chemistry, Graduate Program, Faculty of Mathematics and Natural Sciences, Sebelas Maret University, Surakarta, 57126, Indonesia.

[b] Department of Chemistry, Faculty of Mathematics and Natural Sciences, Sebelas Maret University, Surakarta, 57126, Indonesia.

*Author for correspondence; e-mail: sentotbr@staff.uns.ac.id

Received: 8 March 2020
Revised: 21 April 2020
Accepted: 22 April 2020

ABSTRACT

Two new complexes, Cu(II)-2-amino-6-methylpyridine and Cu(II)-(6-methyl-pyridin-2-ylamino)-acetic acid, were synthesized and characterized to find out the effect of polarity, active groups and complexation on antibacterial activity. The novel ligand, (6-methyl-pyridin-2-ylamino)-acetic acid was synthesized through the rapid and straightforward reaction of 2-amino-6-methylpyridine with chloroacetic acid in less than one minute. Complex of Cu(II) with 2-amino-6-methylpyridine was prepared from the reaction of $CuCl_2 \cdot 2H_2O$ and 2-amino-6-methylpyridine in a mole ratio of 1: 4 in methanol. Complex of Cu(II) with (6-methyl-pyridin-2-ylamino)-acetic acid was synthesized through the reaction of $CuCl_2 \cdot 2H_2O$ and (6-methyl-pyridin-2-ylamino)-acetic acid in a 1:2 mole (metal:ligand) ratio in methanol. The conductivity of all complexes showed a ratio of 1: 2 cations/anions. The proposed formula of the complexes are $[Cu(2\text{-amino-6-methylpyridine})_4]Cl_2 \cdot 2H_2O$ and $[Cu((6\text{-methyl-pyridin-2-ylamino})\text{-acetic acid})_2]Cl_2 \cdot H_2O$. 2-amino-6-methylpyridine is coordinated to Cu(II) via the N-H group, while, (6-methyl-pyridin-2-ylamino)-acetic acid through the carboxylic group. Both complexes were paramagnetic and are expected to have square planar geometry. $[Cu((6\text{-methyl-pyridin-2-ylamino})\text{-acetic acid})_2]Cl_2 \cdot H_2O$ inhibited the highest antibacterial activity.

Keywords: copper(II), pyridines, ligands, square planar, antibacterial

1. INTRODUCTION

Research and discovery of new antimicrobial agents are one of the interests among the scientist [1]. According to the World Health Organization, resistance to multiple antibiotics is now becoming a global problem [2]. Research to find new compounds as antibacterial agents against *Pseudomonas aeruginosa*, *Escherichia coli* and *Staphylococcus aureus* (MRSA) are now imperative [3]. In the last decade, numerous copper(II) complexes have been synthesized, and their antimicrobial activity has been promising [4,5]. Various ligands have been reported, and their coordination with copper seems to enhance their antimicrobial activity [6,7].

2-amino-6-methylpyridine (L1) is a nitrogen donor chelator. Pyridine derivatives are often utilized as ligand due to strongly bind to metal(II)

[8], easy derivatization [9] and having antibacterial activity [10,11]. Several studies have shown that the antibacterial activity of organic compounds can be maximized by optimizing the addition of active groups. Antibacterial activity of 2-aminopyridine was improved by the addition of carboxylic groups resulting in 2,6-pyridinecarboxylic acid [12]. Another compound, 4-methoxy-pyridine-carboxylic acid, had better antibacterial activity than picolinic acid [13]. Besides, the polarity of the compound plays a vital role in antibacterial activity. Hydrophobicity can facilitate penetrating bacteria membrane, thus inhibit the growth of bacteria in vitro [14]. However, the more hydrophobic a compound is, the less it remains in solution of cytoplasm or to stay at a very high concentration due to binding to any proteins and lipids [15]. Thus, water soluble-compounds are preferable for pharmacological applications [16].

In this present work, (6-methyl-pyridin-2-ylamino)-acetic acid, Cu(II)-(6-methyl-pyridin-2-ylamino)-acetic acid and Cu(II)-2-amino-6-methylpyridine complex were synthesized. (6-methyl-pyridin-2-ylamino)-acetic acid is a novel ligand. Derivatization of 2-amino-6-methylpyridine (L1) into (6-methyl-pyridin-2-ylamino)-acetic acid) (L2) by polarity control and the addition of donor atoms are expected to increase the antibacterial activity (Figure 1). Generally, many kinds of organic ligands were synthesized through the reaction of amine groups and chloride acid. However, purification processes were required, including solvent washing, recrystallization, liquid extraction, or column chromatography [17]. L2 was synthesized through a rapid and straightforward method even with facile purification. The influence of particular characteristics of the ligands and corresponding copper(II) complexes in their antibacterial activity was also studied against five antibacterial strains.

2. MATERIALS AND METHODS

2.1 Materials

All the chemicals and solvents used were of reagent grade and chemically pure.

2.2 Synthesis of (6-methyl-pyridin-2-ylamino)-acetic acid (L2)

Chloroacetic acid solution (0.472 g; 5 mmol) in ethyl acetate (10 mL) was dropped into a solution of 2-amino-6-methylpyridine (L1) (0.540 g; 5 mmol) in ethyl acetate (20 mL). The mixture was stirred at room temperature for less than one minute until white precipitate was formed. The product was filtered, washed with ethyl acetate and dried in a vacuum desiccator. The reaction was monitored by thin-layer chromatography (eluent ethyl acetate: n-hexane = 8:1). The obtained compound was analyzed by ^{1}H- and ^{13}C-NMR.

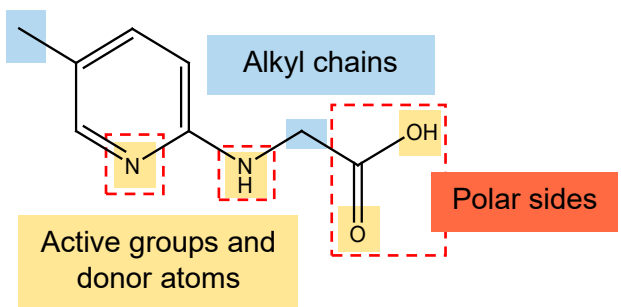

Figure 1. Characteristics of L2.

2.3 Mole-ratio Method in Determining Metal-Ligand Stoichiometry

The determination of Cu(II)-L1 and Cu(II)-L2 coordination number was done by mole ratio method. A series of 0.1 M metal-ligand solutions were prepared from the mixture of methanolic solution of $CuCl_2 \cdot 2H_2O$ and methanolic solution of each ligand with a mole ratio of metal: ligand= 1:0 to 1:7 as shown in Table 1 and 2. Absorbance of all solutions was recorded using a UV-Vis spectrophotometer.

2.4 Preparation of Cu(II)-L1 Complex

$CuCl_2 \cdot 2H_2O$ (0.341 g; 2 mmol) was dissolved in methanol (10 mL) and then added to the L1 solution (0.432 g; 2 mmol) in methanol (15 mL). The solution was stirred at 50 ^{o}C for an hour. Solvent was evaporated to half volume. Green solids were filtered and dried in a vacuum desiccator. Color: light green. Yield: 71%. Solubility: soluble in methanol, ethanol.

Table 1. Series of mixtures of $CuCl_2 \cdot 2H_2O$ and L1.

Metal:ligand mole ratio	$CuCl_2 \cdot 2H_2O$		L1	
	Mass of $CuCl_2 \cdot 2H_2O$ (mg)	Volume of methanol (mL)	Mass of L1 (mg)	Volume of methanol (mL)
1 : 0	17.048	5	0	0
1 : 1	17.048	5	10.814	1
1 : 2	17.048	5	21.628	2
1 : 3	17.048	5	32.442	3
1 : 4	17.048	5	43.256	4
1 : 5	17.048	5	54.070	5
1 : 6	17.048	5	68.884	6
1 : 7	17.048	5	75.698	7

Table 2. Series of mixtures of $CuCl_2 \cdot 2H_2O$ and L2.

Metal:ligand mole ratio	$CuCl_2 \cdot 2H_2O$		L2	
	Mass of $CuCl_2 \cdot 2H_2O$ (mg)	Volume of methanol (mL)	Mass of L2 (mg)	Volume of methanol (mL)
1 : 0	17.048	5	0	0
1 : 1	17.048	5	16.618	1
1 : 2	17.048	5	33.236	2
1 : 3	17.048	5	49.854	3
1 : 4	17.048	5	66.472	4
1 : 5	17.048	5	83.090	5
1 : 6	17.048	5	99.708	6
1 : 7	17.048	5	116.326	7

2.5 Preparation of Cu(II)-L2 Complex

$CuCl_2 \cdot 2H_2O$ (0.170 g; 1 mmol) was dissolved in methanol (10 mL) and then added to the L2 solution (0.332 g; 2 mmol) in methanol (15 mL). The mixed solution was stirred for an hour then left overnight at room temperature until precipitates were formed. The precipitate was filtered and dried in a vacuum desiccator. Color: dark green. Yield: 78%. Solubility: soluble in water.

2.6 Physical Measurements

^{1}H-NMR and ^{13}C-NMR data were recorded by an Agilent 500 MHz NMR spectrometer using CD_3OD at room temperature. Copper content in the complex was determined by a Shimadzu AA-6650 Atomic Absorption Spectrophotometer (AAS). Thermal analysis was performed using a Shimadzu 50 Differential Thermal Analyzer with a heating rate of 10 °C/min. Molar conductivity was measured at 25 °C on a Jenway CE 4071 conductivity meter, having a dip type cell calibrated with KCl solution. Infrared spectra were measured on a Prestige-21 Shimadzu spectrophotometer as KBr pellets in the frequency range of 4000–450 cm^{-1}. UV-VIS spectra were obtained using a Shimadzu PC 1601 UV-Vis Double Beam spectrophotometer. Susceptibility values of the copper complexes were recorded using an Auto Sherwood Scientific 10169 Magnetic Susceptibility Balance. The diamagnetic corrections were made by using Pascal's constants.

2.7 Antibacterial Test

Investigation of antibacterial activity used disk-diffusion method. Bacterial suspension of *Staphylococcus aureus, Staphylococcus epidermidis, Escherichia coli, Salmonella typhi* dan *Pseudomonas aeruginosa* was prepared by dissolving single colony of each bacterium in NaCl 0.09%. Each bacterial suspension was smeared to the surface of Mueller-Hinton agar and incubated for 10 minutes in an oven at 37 °C. Each 6 mm blank disk was dropped with 15 microliters of sample extracts in DMSO with concentrations of 7.5; 15; 30; and 45 µg/disk. Negative control was carried out on DMSO, and positive control was also carried out using antibiotics. The disks were placed regularly on the agar media and incubated at ± 37 °C. After 24 hours, clear zone diameter around the disks was measured. The inhibition zone was measured using Krisbow electronic callipers with a precision of ± 0.01 mm.

3. Results and Discussion

3.1 Synthesis of L2

In this investigation, L2 synthesis was performed simply through a facile reaction. Pure L2 was obtained by reaction of L1 with chloroacetic acid in a mole ratio of 1: 1 at room temperature. A plausible reaction is shown in Figure 2. The choice of the solvent was crucial. The reactants were highly soluble in ethyl acetate, while, the product has poor solubility in it. Therefore, the

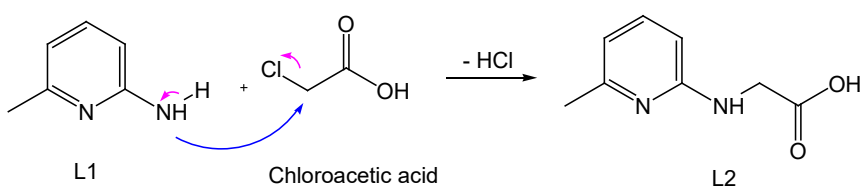

Figure 2. Plausible reaction of L2 synthesis.

product immediately precipitated from the solution with high yield. Temperature also plays a role in the reaction. Due to the reactivity of chloride and amine groups, the reaction was rapid and therefore carried out without heating to avoid side products. The ligand is highly soluble in water and alcohols.

FTIR spectrum of L2 showed absorptions band at 1674 and 1632 cm^{-1} corresponding to the vibration of C=O and C=N, as shown in Figure 3. The changes in N-H absorption profile from two sharp peaks in L1 into broad peaks in L2 at around 3305 cm^{-1} indicated the release of one hydrogen atom and the change of NH_2 into NH-C. ^{1}H-NMR data of L2 shows several proton environments (Figure 4), ^{1}H-NMR (500 MHz, CD_3OD): δ 7.71 (J = 8.9, 7.2 Hz); 6.74; 6.62; 5.06; 4.03; 2.46 ppm. Chemical shift values indicate six asymmetric protons of the product in the range of 2.46-7.71 ppm. Singlet peaks at 2.46 and 4.03 ppm were corresponding to methyl and ethyl proton of L2. A peak of proton of NH was found at 5.06 ppm. Three peaks at 6.62, 6.74, and 7.71 ppm were corresponding to aromatic protons. Proton of solvent also appeared at 3.32 ppm. Carboxylic proton was not shown in the spectrum. Labile proton often cannot be detected. In the ^{13}C NMR spectrum shown in Figure 5, eight peaks were found relevant to the expected structure, among others ^{13}C NMR (125 MHz, CD_3OD) δ 173.56 (1C, COOH); 155.58 (1C, Ar-C); 147.69 (1C, Ar-C); 143.48 (1C, Ar-C); 111.42 (1C, Ar-C), 109.59 (1C, Ar-C); 43.16 (1C, CH_2);17.86 (1C, CH_3). Carbon atoms of the solvent were detected at 47.63 ppm.

3.2 Mole-ratio Method in Determining Metal-Ligand Stoichiometry

UV-Vis spectra of Cu(II)-L1 and Cu(II)-L2 solutions with different mole ratio of metal to ligand is presented in Figures 6 and 7. UV-vis spectra of the mixture solution exhibit blueshift by the addition of the ligand. The graphs of maximum wavelength vs mole ratio (Figures 8 and 9) reveal that the maximum wavelength becomes stable in the ratio of Cu(II): L1 = 1:4 and Cu(II): L2 = 1:2. It indicates that four moles of L1 and two moles

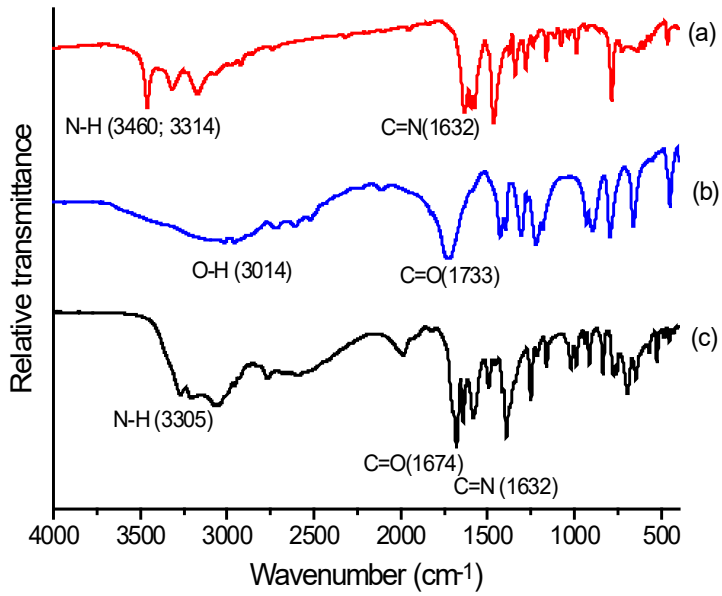

Figure 3. IR spectra of L1 (a), chloroacetic acid (b) and L2 (c).

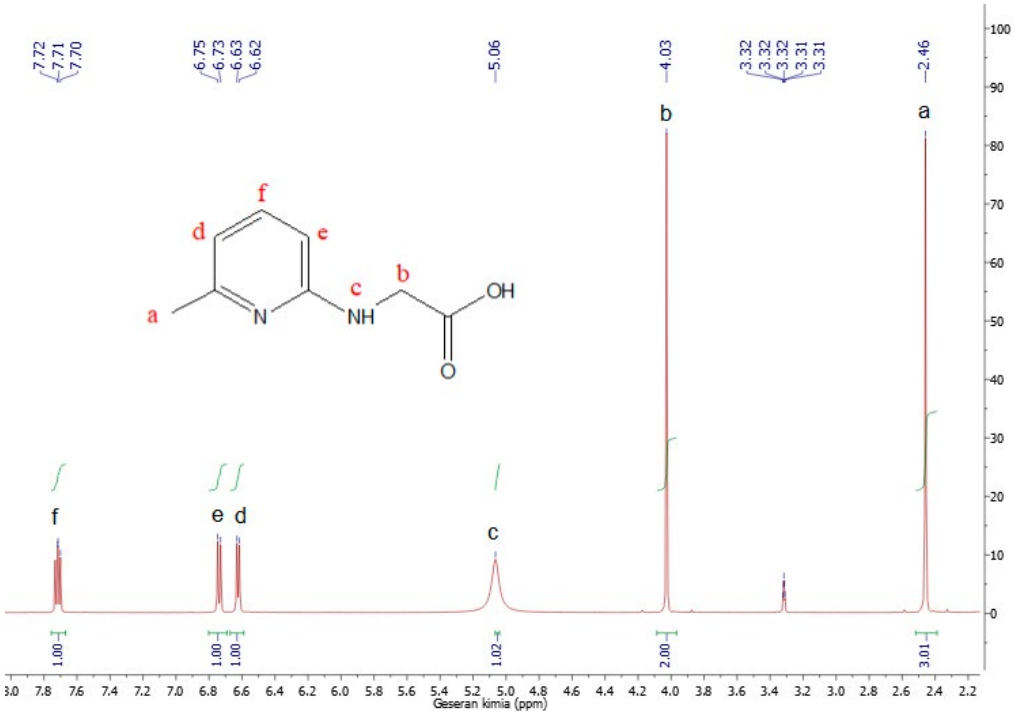

Figure 4. [1]H-NMR spectrum of L2.

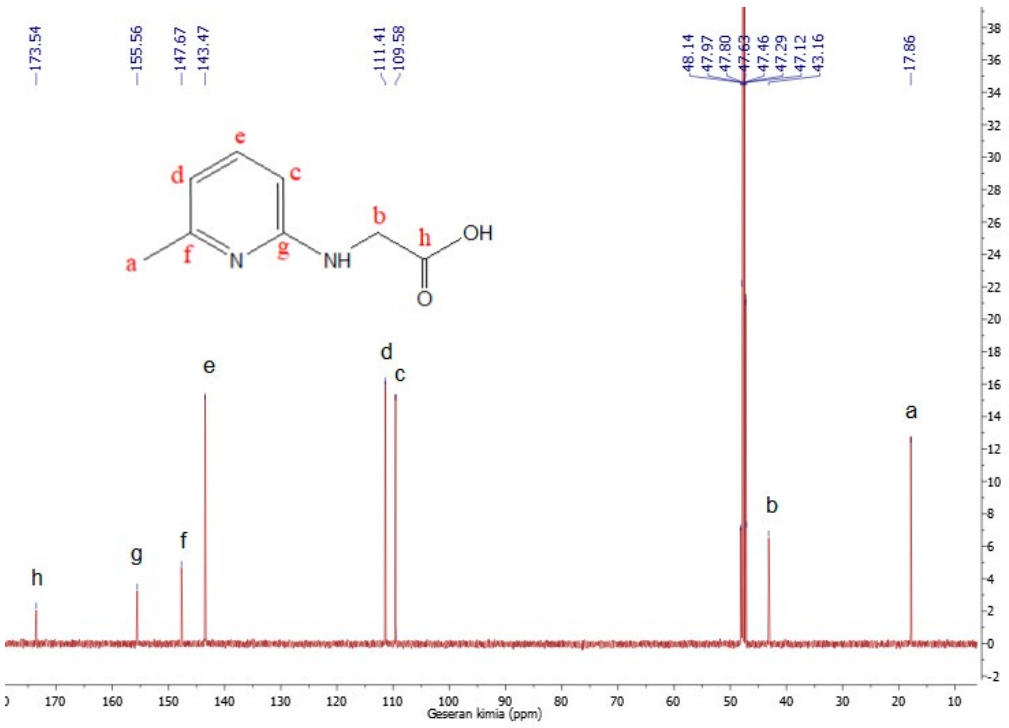

Figure 5. [13]C-NMR spectrum of L2.

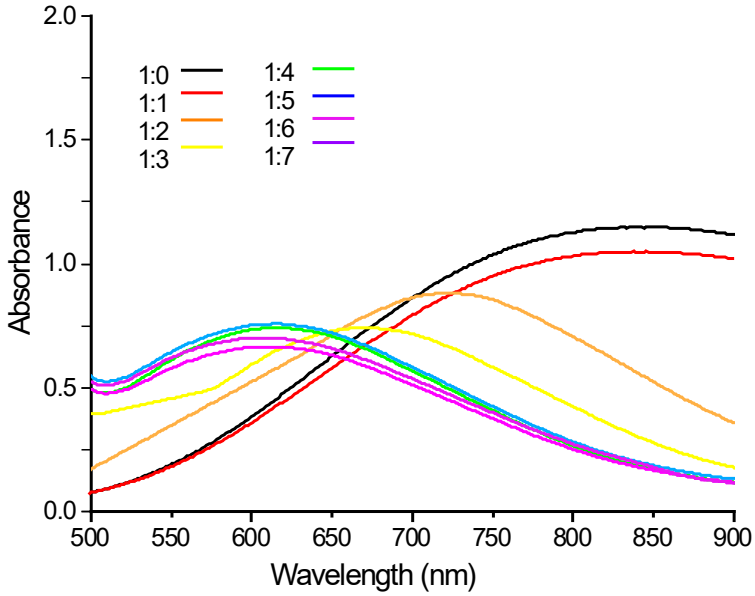

Figure 6. UV-Vis spectra of Cu(II)-L1 with mole ratio (metal:ligand) of 1:0 until 1:7.

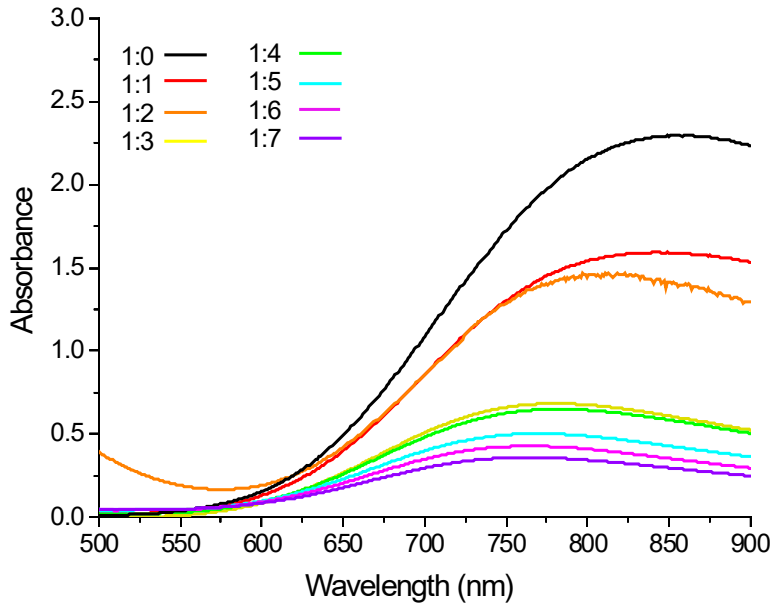

Figure 7. UV-Vis spectra of Cu(II)-L2 with mole ratio (metal:ligand) of 1:0 until 1:7.

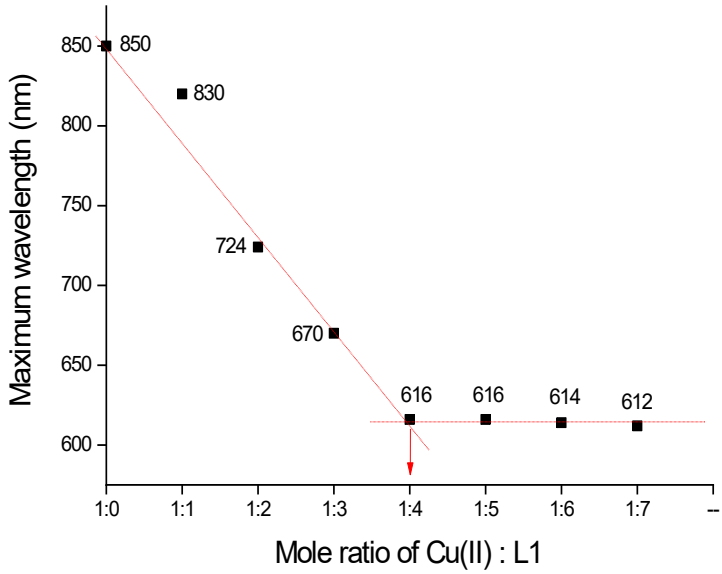

Figure 8. Determination of Cu(II)-L1 coordination number.

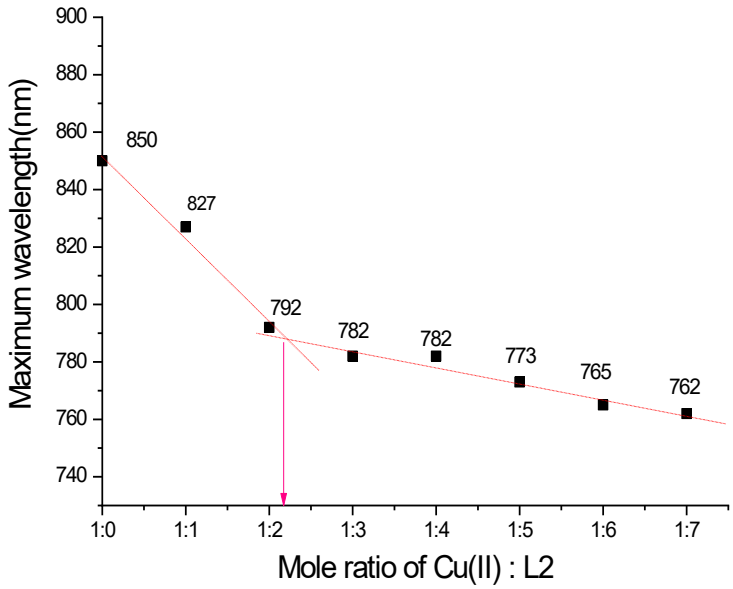

Figure 9. Determination of Cu(II)-L2 coordination number.

of L2 can replace water molecules and coordinate with Cu(II).

3.4 AAS Result of Cu(II)-L1 and Cu(II)-L2

Empirical formula of the complex was determined by comparing the percentage of copper in the complex with the calculated copper content in several possible complex formulas. Table 3 and 4 explains that the possible formula for the Cu(II)-L1 and Cu(II)-L2 complex is $Cu(L1)_4Cl_2(H_2O)_x$, x=1, 2, or 3 and $Cu(L2)_2Cl_2(H_2O)_x$, x=1, 2, or 3.

3.5 TGA-DSC (Thermogravimetric Analysis-Differential Scanning Calorimetry)

Cu(II)-L1 shows 5.87% one step of mass loss from 32-150 °C (Figure 10). It indicates a release of two molecules of water (calculated: 5.97%). DSC curve also shows an endothermic peak at 119 °C, which is associated with the evaporation of lattice water. The TG curve of Cu(II)-L1 also shows two steps of weight loss of 66.88% (calculated: 71.71%) in the range 150-541 °C, which is attributable to the phase transition and dissociation of four molecules of L1. Therefore, empirical formula of Cu(II)-L1 is $Cu(L1)_4Cl_2H_2O$. The TG of Cu(II)-L2 complex indicates a weight loss of 3.75% (calculated: 3.71 %), which is observed in a single step in the temperature range of 35-110 °C (Figure 11). It is assigned to the loss of a molecule of water. The DSC curve of this complex shows a short endothermic peak around 95 °C. Other peaks at around 110 and 531 °C may be due to some phase transition and decomposition of organic molecules, followed by a weight loss of 67.03 %. It indicates the loss of four molecules of L2 (calculated: 68.54%). From the data, the empirical formula of Cu(II)-L2 is $Cu(L2)_2Cl_2(H_2O)_2$. Both complexes show mass reduction continuing up to 600 °C. From the thermogram, it is expected that the complexes achieve stability to produce CuO residue at temperatures over 600 °C.

3.6 Conductivity

Molar conductivity of Cu(II)-L1 was taken in methanol, and Cu(II)-L2 in water. According to Table 5 and Table 6, Cu(II)-L1 and Cu(II)-L2 have molar conductivity of 105 $S.cm^2/mol$ and 271 $S.cm^2/mol$, respectively. It indicates that both complexes are electrolytes with a 1:2 mole ratio of cation/anion [18]. Chloride ions acted as counter ions and not coordinated to the central metal ion. Thus, the formula of two complexes is $[Cu(L1)_4]Cl_2{\cdot}2H_2O$ and $[Cu(L2)_2]Cl_2{\cdot}H_2O$, namely, tetrakis-

Table 3. Copper content in Cu(II)-L1.

Complex formulas	Calculated copper content (%)	AAS result (%)
$Cu(L1)_4Cl_2H_2O$	10.86	
$Cu(L1)_4Cl_2(H_2O)_2$	10.53	10.55 ± 0.13
$Cu(L1)_4Cl_2(H_2O)_3$	10.23	

Table 4. Copper content in Cu(II)-L2.

Complex formulas	Calculated copper content (%)	AAS result (%)
$Cu(L2)_2Cl_2H_2O$	13.10	
$Cu(L2)_2Cl_2(H_2O)_2$	12.63	12.84 ± 0.07
$Cu(L2)_2Cl_2(H_2O)_3$	12.19	

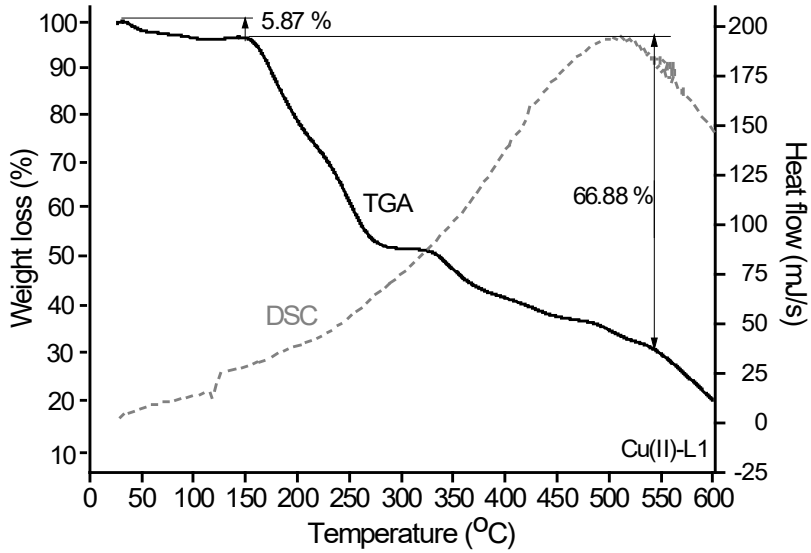

Figure 10. TGA-DSC thermogram of Cu(II)-L1.

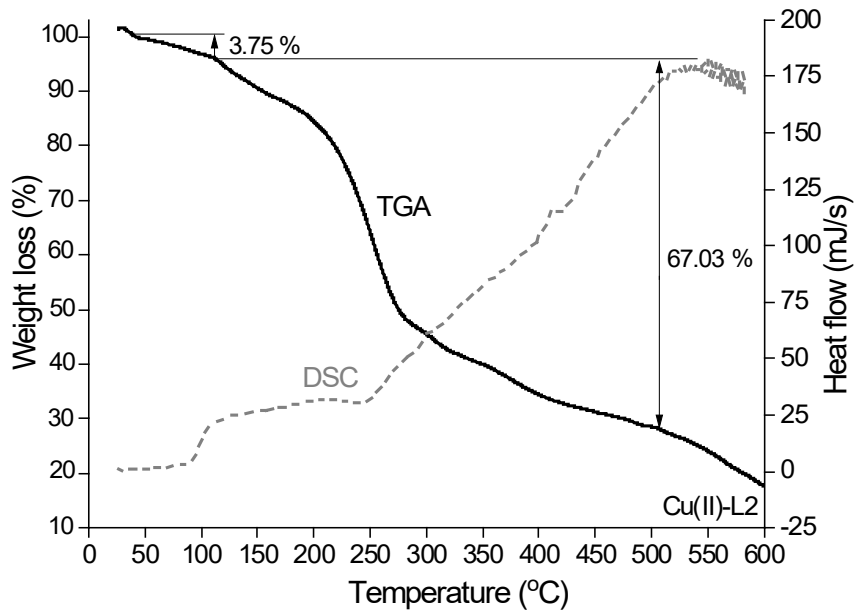

Figure 11. TGA-DSC thermogram of Cu(II)-L2.

Table 5. Conductivity of Cu(II)-L1 and known salts in methanol.

Compounds	Conductivity (μs/cm)	Molar conductivity ($S.cm^2/mol$)	Cation/anion ratio	Number of ions
Methanol	2 ± 0	2	-	-
$CuSO_4 \cdot 5H_2O$	2 ± 0	2	1:1	2
$FeSO_4 \cdot 7H_2O$	12 ± 0.4	12	1:1	2
$NiCl_2 \cdot 6H_2O$	92 ± 0.4	92	2:1	3
$CoCl_2 \cdot 6H_2O$	107 ± 0.6	107	2:1	3
$Fe(NO_3)_3 \cdot 9H_2O$	144 ± 1.5	144	3:1	4
Cu(II)-L1	105 ± 0.5	105	2:1	3

Table 6. Conductivity of Cu(II)-L2 and known salts in water.

Compounds	Conductivity (μs/cm)	Molar conductivity ($S.cm^2/mol$)	Cation/anion ration	Number of ions
Akuades	8	8	-	-
$FeSO_4 \cdot 7H_2O$	116 ± 1.1	116	1:1	2
$CuSO_4 \cdot 5H_2O$	133 ± 1	133	1:1	2
$CoCl_2 \cdot 6H_2O$	270 ± 2	270	2:1	3
$NiCl_2 \cdot 6H_2O$	283 ± 1.1	283	2:1	3
$CuCl_2 \cdot 2H_2O$	314 ± 0	314	2:1	3
Cu(II)-L2	271 ± 2	271	2:1	3

2-amino-6-methylpyridine acid copper(II) chloride dihydrate and di-6-methyl-2-amino-yl-acetic acid copper(II) chloride monohydrate.

3.7 Infrared Spectra

FTIR spectra of L1 and Cu(II)-L1 are given in Figure 12. FTIR spectrum of free L1 shows two sharp peaks at 3460 and 3314 cm^{-1} assigned to ν(N-H). FTIR spectrum of Cu(II)-L1 reveals the presence of peaks at 3312 and 3356 cm^{-1}, which can be assigned to ν(N-H). These positive and negative shifts indicate the coordination of N-H [19]. Absorption at 1632 cm^{-1} attributed to ν(C=N) is found to be almost unchanged in Cu(II)-L1 ruling out the possibility of C=N pyridine taking part in the chelation.

FTIR spectrum of free L2 shows some absorption at 3305; 3115 (νN-H); 1674; 1403 (νC=N) and 1632 (νCOO) cm^{-1} (Figure 13). The upward shift of ν(COO) to 1697;1425 cm^{-1} in Cu(II)-L2 indicate the coordination of COO to the metal ion [20]. There is no change in wavenumbers of C=N and N-H, indicating the two groups are not involved in coordination.

3.8 Electronic Spectra

UV-vis spectra of Cu(II)-L1 and Cu(II)-L2 were recorded in methanol and water, respectively. Electronic spectral data of $CuCl_2 \cdot 2H_2O$, Cu(II)-L1, and Cu(II)-L2 are shown in Table 7. Both complexes exhibit blueshift compared to $CuCl_2 \cdot 2H_2O$, as shown in Figure 14. It reveals that the ligands can change water molecules in Cu(II) solution. The maximum wavelength shifted from 850 nm ($CuCl_2 \cdot 2H_2O$) to 616 nm (ε: 4.2) for Cu(II)-L1 and from 814 nm ($CuCl_2 \cdot 2H_2O$) to 775 nm (ε: 9.0) for Cu(II)-L2. The maximum wavelength of both complexes appeared as single broad absorption,

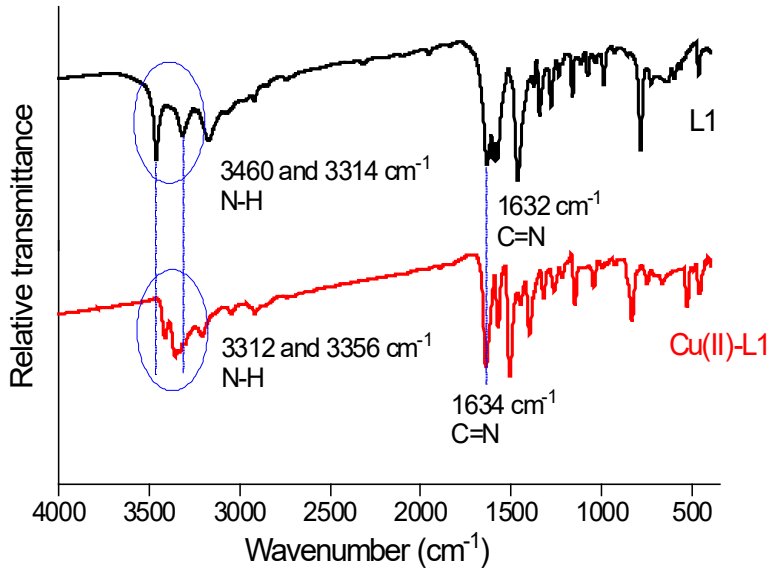

Figure 12. IR spectra of L1 and Cu(II)-L1.

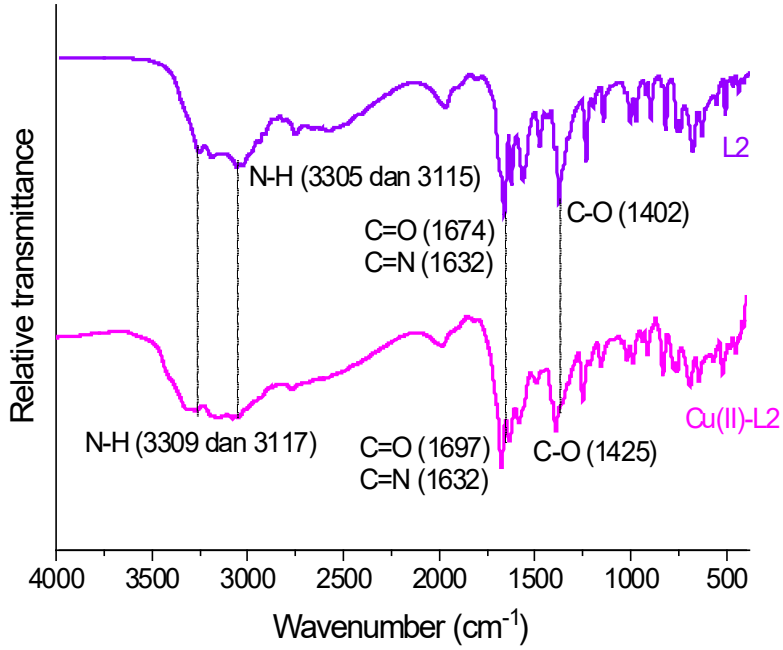

Figure 13. IR spectra of L2 and Cu(II)-L2.

Table 7. Electronic spectral data of $CuCl_2 \cdot 2H_2O$, Cu(II)-L1, dan Cu(II)-L2 with concentration of 10^{-2} M.

Compounds	λ_{max}(nm)	A	ν (cm^{-1})	ε (L/mol.cm)	Solvent
$CuCl_2 \cdot 2H_2O$	850	0.124	11,764	12.4	Methanol
Cu(II)-L1	616	0.042	14,814	4.2	Methanol
$CuCl_2 \cdot 2H_2O$	814	0.165	12,228	16.5	Water
Cu(II)-L2	775	0.090	12,903	9.0	Water

Note: λ_{max}: maximum wavelength in UV-Vis spectra (refers to Figure 14 and 15); A:absorbance; ν: frequency; ε: molar absorptivity;

which can be assigned to $^2B_{1g} \rightarrow {}^2A_{1g}$ and $^2B_{1g} \rightarrow {}^2B_{2g}$, respectively. Square planar geometries exhibit the absorption bands corresponding to $^2B \rightarrow {}^2A_{1g}$, $^2B_{1g} \rightarrow {}^2B_{2g}$ and $^2B_{1g} \rightarrow {}^2E_g$) [21]. Square planar Cu(II) complexes often give a broad absorption, due to Jahn–Teller (J–T) distortions, generally only one broad band is observed [22]. Thus, it is expected that both copper(II) complexes have square planar geometry.

3.9 Magnetism

The measurements were done using three samples of each complex with different mass at temperature of 300K. The average effective magnetic moment (μ_{eff}) of Cu(II)-L1 and Cu(II)-L2 was 1.82 and 1.85 BM, which indicated one unpaired electron. Therefore, the results reveal that the complexes are paramagnetic. The μ_{eff} value also supports that the complex has a square planar geometry [23]. From all characterization data, the proposed structure of $[Cu(L1)_4]Cl_2 \cdot 2H_2O$ and $[Cu(L2)_2]Cl_2 \cdot H_2O$ is presented in Figures 16 and 17.

3.10 Antibacterial Activity

Antibacterial activity of metals, ligands, complexes, and standards are presented in Table 8. In general, all compounds at concentrations of more than 7.5 μg/disk show antibacterial activity. The highest activity for all concentrations and all bacteria was Cu(II)-L2, followed by Cu(II)-L1 > $CuCl_2 \cdot 2H_2O$ > L2 > L1. Antibacterial activity of commercial antibiotics (positive standards) are still higher then tested compounds. However, the antibacterial activity of L1 increases for all bacteria when modified into L2. This improvement is due to having more active groups. L1 contains C=N and NH_2 groups as active groups, and L2 contains C=N, N-H, and COOH groups, which can bind to hydrogen of groups on cell membranes and bacterial proteins. Penetration of ligands into bacterial cells also causes lysis.

The complex has a higher antibacterial activity than the metal and its ligands. It proves that complexing can increase the antibacterial activity. Inhibitory test results show that metals and ligands work in synergy after complexing. The lipid membrane surrounding the cell wall of bacteria is non-polar [4]. One of the most important factors for controlling antibacterial activity is lipophilicity. Following Tweedy's chelation theory and Overtone's concept, coordination bonds can reduce the polarity of metal ions due to partial cation sharing with donor atoms and delocalization of electrons π across the chelate ring [24]. This coordination enhances the lipophilic character and supports permeation through the lipid layer of the bacterial membrane. This process can block the enzymatic activity of cells that stop the process of respiration of microorganisms [8]. However, the cytoplasm contains water. Polarity also plays a role in antibacterial activity after penetration to

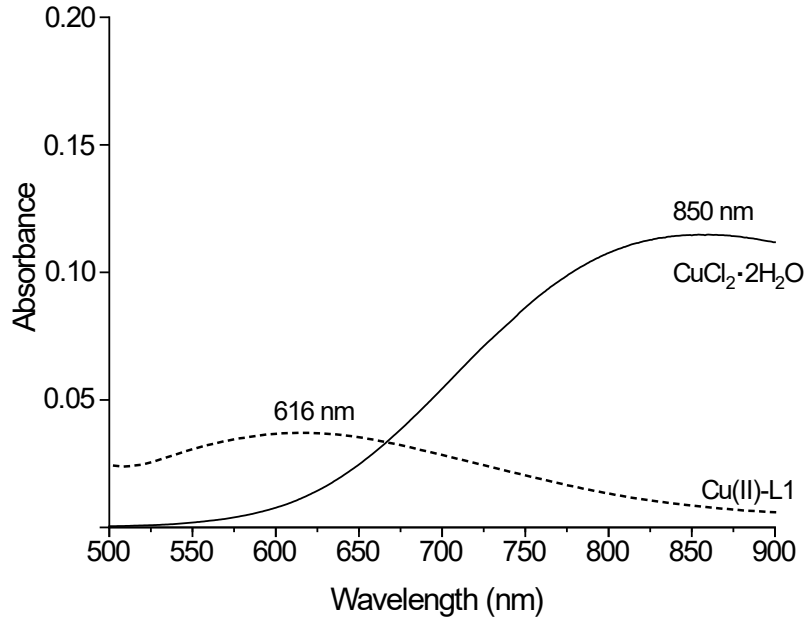

Figure 14. UV-Vis spectra of $CuCl_2 \cdot 2H_2O$ and Cu(II)-L1 in methanol.

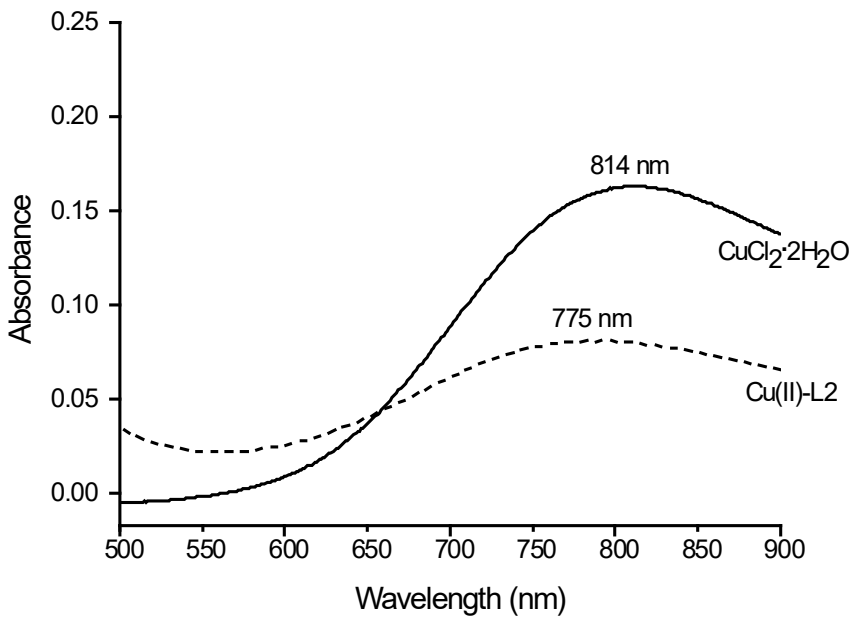

Figure 15. UV-Vis spectra of $CuCl_2 \cdot 2H_2O$ and Cu(II)-L2 in water.

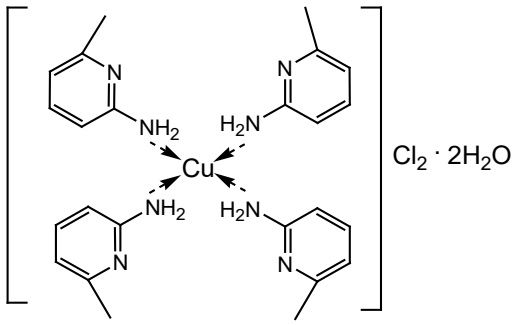

Figure 16. Proposed structure of $[Cu(L1)_4]Cl_2 \cdot 2H_2O$.

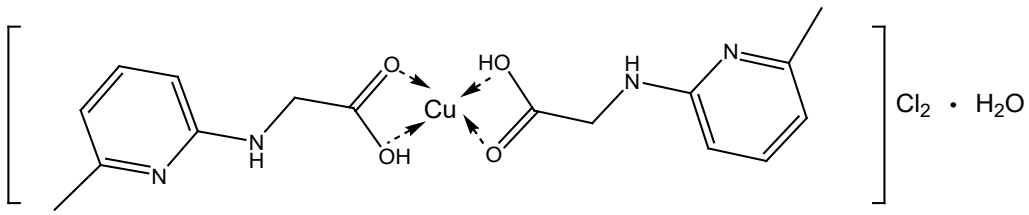

Figure 17. Proposed structure of $[Cu(L2)_2]Cl_2 \cdot H_2O$.

membrane cells. Hydrophobic compounds can easily penetrate bacteria membrane, thus inhibit the growth of bacteria in vitro [25, 26]. However, the more hydrophobic a compound is, the less it remains in solution of cytoplasm or to stay at a very high concentration due to binding to any proteins and lipids [27]. Thus, water soluble-compounds are desired for pharmacological applications [15].

The Cu(II)-L2 have higher activity than Cu(II)-L1. Complexes with bidentate ligands have higher antibacterial activity than complexes with monodentate ligands [28] L2 can contribute electrons to the metal, thereby increasing the lipophilic nature of the central metal. Cu(II)-L2 more easily enters the bacterial cell membrane. In bacterial cell membranes, there are active groups such as carboxyl, phosphoryl, and amino. The COOH groups in Cu(II)-L2 have low ligand field strength according to the spectrochemical sequence [29]. COOH groups can be replaced by other functional groups in cell membranes, proteins, and bacterial DNA. Besides, uncoordinated active groups of L2 can bond hydrogen with active groups on bacteria so that the mechanism of action becomes diverse [30]. This feature resulted in increased antibacterial activity.

4. Conclusions

L2 was successfully synthesized from L1 with rapid and facile method. L1 was monodentate ligand through coordination of N-H, and L2 was bidentate ligand through the carboxylate group. Moment magnetic measurements reveal both complexes are paramagnetic. Antibacterial

Table 8. Inhibition zone (mm) of observed compounds against Gram-positive and Gram- negative bacteria.

Compounds	Concentration (µg/disk)			
	7.5	15	30	45
Staphylococcus aureus				
$CuCl_2 \cdot 2H_2O$	-	7.85	8.27	9.35
L1	-	6.87	7.46	7.63
Cu(II)-L1	-	7.94	8.32	10.11
L2	-	7.11	7.91	8.82
Cu(II)-L2	-	8.57	10.97	11.87
Staphylococcus epidermidis				
$CuCl_2 \cdot 2H_2O$	-	7.73	9.12	12.19
L1	-	-	-	-
Cu(II)-L1	-	8.25	11.17	12.68
L2	-	-	-	7.53
Cu(II)-L2	-	9.07	13.44	15.96
Pseudomonas aeruginosa				
$CuCl_2 \cdot 2H_2O$	-	7.14	7.76	8.81
L1	-	6.82	7.14	7.43
Cu(II)-L1	-	7.76	8.23	8.83
L2	-	7.31	7.80	8.27
Cu(II)-L2	-	8.11	9.55	11.42
Escherichia coli				
$CuCl_2 \cdot 2H_2O$	-	7.65	8.24	10.32
L1	-	-	6.91	7.45
Cu(II)-L1	-	7.28	8.36	10.83
L2	-	7.00	7.87	8.62
Cu(II)-L2	-	8.26	11.29	13.51
Salmonella typhi				
$CuCl_2 \cdot 2H_2O$	-	-	7.64	8.35
L1	-	-	-	7.03
Cu(II)-L1	-	-	8.33	9.96
L2	-	-	-	7.00
Cu(II)-L2	-	8.25	9.37	11.04

Note: L1: 2-amino-6-methylpyridine; L2: (5-methyl-pyridin-2-ylamino)-acetic acid; Antibiotics used for *St. aureus*: vancomycin; *St. epidermidis:* clindamycin; *P. aeruginosa*: gentamycin; *E. coli:* chloramphenicol; *S. thypi*: amoxicillin. Inhibition zone was measured in millimeter.

activity of complexes was better than $CuCl_2 \cdot 2H_2O$ and ligands. Modification of L1 into L2 and complexation with copper seems to be promising to increase the antibacterial activity.

Acknowledgment

The authors express acknowledgments to Sebelas Maret University for financial support through Hibah Penelitian Fundamental PNBP UNS.

References

[1] Cote C., Blanco I., Hunter M., Shoe J., Klimko C., Panchal R. and Welkos S., *Microb. Pathogenesis*, 2020; **142**: 104050. DOI 10.1016/j.micpath.2020.104050.

[2] World Health Organization, Antimicrobial Resistance: Global Report on Surveillance; Available at: https://apps.who.int/iris/bitstream/10665/112642/1/9789241564748_eng.pdf.

[3] Dokla E.M., Abutaleb N.S., Milik S.N., Li D., El-Baz K., Shalaby M.W., Al-Karaki R., Nasr M., Klein C.D., Abouzid K.A.M. and Seleem M.N., *Eur. J. Med. Chem.*, 2020; **186**: 111850. DOI 10.1016/j.ejmech.2019.111850.

[4] Albobaledi Z., Hasanzadeh M.E., Behzad M. and Abbasi A., *Inorg. Chim. Acta*, 2020; **499**: 119185. DOI 10.1016/j.ica.2019.119185.

[5] Arif R., Nayab P.S., Ansari I.A., Shahid M., Irfan M., Alam, S., Abid M. and Rahisuddin, *J. Mol. Struct.*, 2018; **1160**: 142-153. DOI 10.1016/j.molstruc.2018.02.008

[6] Vamsikrishna N., Daravath S., Ganji N., Pasha N. and Shivaraj, *Inorg. Chem. Commun.*, 2020; **113**: 107767. DOI 10.1016/j.inoche.2020.107767.

[7] Scriven E. and Murugan R., *Kirk-Othmer Encyclopedia of Chemical Technology*, 2000; DOI 10.1002/0471238961.1625180919031809.a01.pub2.

[8] Raghavulu K., Sambaiah M., Gudipati R., Basavaiah K., Yennam S. and Behera M., *J. Saudi Chem. Soc.*, 2019; **23(8)**: 1024-1031. DOI 10.1016/j.jscs.2019.05.008.

[9] Radwan M.A., Alshubramy M.A., Abdel-Motaal M., Hemdan, B.A. and El-Kady D.S., *Bioorg. Chem.*, 2020; **96**: 103516. DOI 10.1016/j.bioorg.2019.103516.

[10] Bhardwaj V., Noolvi M.N., Jalhan S., and Patel H.M., *J. Saudi Chem. Soc.*, 2016; 20: S406-S410. DOI 10.1016/j.jscs.2012.12.007.

[11] Nayak S.G., and Poojary, B., *Heliyon*, 2019; **5(8)**: e02318. DOI 10.1016/j.heliyon.2019.e02318.

[12] Yenikaya C., Poyraz M., Sarı M., Demirci F., İlkimen H. and Büyükgüngör O., *Polyhedron,* 2009; **28(16)**: 3526-3532. DOI 10.1016/j.poly.2009.05.079.

[13] Tamer Ö., Tamer S., İdil Ö., Avcı D., Vural H. and Atalay Y., *J. Mol. Struct.* 2018; **1152**: 399-408. DOI 10.1016/j.molstruc.2017.09.100.

[14] Lopez-Romero J.C., González-Ríos H., Borges A. and Simões M. *Evid.-Based Compl. Alt.*, 2015; **2015**: 1-9: DOI 10.1155/2015/795435.

[15] Basarab G.S, Eakin A.E. and Nichols W.W., Design of Antibacterial Agents; in Tang Y., Sussman M., Liu D., Poxton I. and Schwartzman J., eds., *Molecular Medical Microbiology*, Academic Press, Cambridge, 2015: 611-626.

[16] Savjani K.T., Gajjar A.K., and Savjani J.K., *ISRN Pharm.*, 2012; **2012**: 1-10. DOI 10.5402/2012/195727.

[17] Bousfield T.W., Pearce K.P., Nyamini S.B., Angelis-Dimakis A., and Camp J.E., *Green Chem.*, 2019; **21(13)**: 3675-3681. DOI 10.1039/c9gc01180c.

[18] Shirvan A., Golchoubian H. and Bouwman E., *J. Mol. Struct.*, 2019; 1195: 769-777. DOI 10.1016/j.molstruc.2019.06.034.

[19] Yousef T. and Abu El-Reash G., *J. Mol. Struct.*, 2020; **1201**: 127180. DOI 10.1016/j.molstruc.2019.127180.

[20] Muhammad N., Ikram M., Perveen F., Ibrahim M., Ibrahim M., Abel V., Rehman S., Shujah S., Khan W., Shams D.F. and Schulzke C., *J. Mol. Struct.*, 2019; **1196**: 771-782. DOI 10.1016/j.molstruc.2019.07.014.

[21] Ahmed A. and Lal R.A. *Arab. J. Chem.*, 2017; **10**: S901-S908. DOI 10.1016/j.arabjc.2012.12.026.

[22] Do Prado J.F., Valdo A.K., Martins F.T., De Santana R.C. and Cangussu D., *J. Mol. Struct.*, 2020; **1203**: 127468. DOI 10.1016/j.molstruc.2019.127468.

[23] Ispir E., Ikiz M., Inan A., Sünbül A.B., Tayhan S.E., Bilgin S., Köse M. and Elmastaş M., *J. Mol. Struct.*, 2019; **1182**: 63-71. DOI 10.1016/j.molstruc.2019.01.029.

[24] Fousiamol M., Sithambaresan M., Damodaran K.K. and Kurup M.P., *Inorg. Chim. Acta*, 2020; **501**: 1193 01. DOI 10.1016/j.ica.2019.119301.

[25] Kuroda K., Caputo G. and DeGrado W., *Chem. Eur. J.*, 2008; **15(5)**: 1123-1133. DOI 10.1002/chem.200801523.

[26] Lopez-Romero J.C., González-Ríos H., Borges A. and Simões M., *Evid-Based Compl. Alt.*, 2015; **2015**: 1-9. DOI 10.1155/2015/795435.

[27] Basarab G.S., Eakin A.E. and Nichols W.W., Design of Antibacterial Agents; in Tang Y., Sussman M., Liu D., Poxton I., Schwartzman J., eds., *Molecular Medical Microbiology*, Academic Press, Cambridge, 2015: 611-626.

[28] Rizzotto M., Metal complexes as antimicrobial agents, a Search for antibacterial agents; Available at: https://www.intechopen.com/books/a-search-for-antibacterial-agents/metal-complexes-as-antimicrobial-agents.

[29] Patra S.G. and Datta D., *Comput. Theor. Chem.*, 2018; **1130**: 77-82. DOI 10.1016/j.comptc.2018.03.012.

[30] Jayendran M., Begum P.S. and Kurup M.P., *J. Mol. Struct.*, 2020; **1206**: 127682. DOI 10.1016/j.molstruc.2020.127682.